

# The Performance of Chirp Signal Used in LEO Satellite Internet of Things

Yubi Qian, Lu Ma, Xuwen Liang

**Abstract**—The technology of Chirp Spread Spectrum (CSS) has been developed for decades, widely known to be used in the field of radar and sonar. In recent years, CSS is used in IEEE 802.15.4a and LoRa (Long Range) Internet of Things (IoT) called LoRa modulation. On the other hands, CSS has never been used in Low-Earth-Orbit (LEO) satellite communication systems for low-data-rate transmission (IoT). CSS applied in LoRa as a kind of successful commercial IoT technology will promote us to do research on its application in satellite communication for IoT. There are some new types of chirp signal with the same chirp rate to realize multiple access in these years. Based on these, this letter is on the research of these kinds of chirp signal in satellite multiple access communication systems.

**Index Terms**—CSS, IoT, LEO Satellite, Multiple Access Communication.

## I. INTRODUCTION

Currently, more than 80 percent of the world's land and more than 95 percent of its oceans are not covered by mobile cellular networks. With the development of Low-Earth-Orbit (LEO) satellites in recent years, they can provide reliable communication services for the places where there is no terrestrial network. In terms of power, propagation delay and coverage [1], LEO satellites are more suitable for IoT communication than other types of satellites. Spread Spectrum Aloha (SSA) [2] [3] with Direct Sequence Spread Spectrum (DSSS) as a kind of Pure ALOHA (PA) which is a type of random access protocol has been proposed for machine-to-machine communication with satellites, and PA is the best choice for satellite Internet of Things (IoT) detailed in [2]. Moreover, PA is applied to LoRa (Long Range) [4] [5] Class-A terminals which have low power consumption. Chirp Spread Spectrum (CSS) [6] [7] as a kind of rapid development of spread spectrum, has never been used in satellite communication for low-data-rate transmission while LoRa has successfully applied it to Low-Power Wide-Area Network [8] in the terrestrial IoT, like data acquisition, position report and so on.

CSS modulation has the characteristics of anti-frequency offset and anti-interference shown in *Sec-IV.A*. In addition, Time Delay (TD) and Doppler Frequency Shift (DFS) of Chirp signal (CS) are easy to be captured shown by those

two acquisition methods in [9] [10], which benefits the low-power design of communication system. In summary, CSS is very suitable for low-data-rate transmission in LEO satellite communication system whose applications are detailed in [3].

In recent years, LoRa Chirp Signal (LCS) [4] has been used in terrestrial IoT and Symmetry Chirp Signal (SCS) [11] was proposed to be used in LEO satellite IoT. In LEO satellite communication, maximum DFS (several  $KHz$  to tens of  $KHz$ ) is much bigger than that in the terrestrial communication, and symbol rate (Hundreds of  $bps$ ) is low in IoT. In this letter, we put forward another kind of Chirp signal called Asymmetry Chirp Signal (ACS) which is a type of revised SCS and has better performance in LEO satellite communication system. In this letter, we mainly compare access performance and acquisition performance of LCS, SCS and ACS.

Following this Introduction, channel model which is simplified to compare those two types of performance is declared in Section II. Then we describe ACS and find that it keeps good auto-correlation comparing with SCS and has better cross-relation in time and frequency domain. Therefore we compare the multiple access performance of ACS, SCS, LCS, Hadamard Matrices and m-Sequences in random access channel in Section III. In Section IV, first of all, we analyse the advantages of CSS applied to satellite communication. Then we express that TD and DFS of CS are easier to be captured than DSSS signal, and comparing SCS, ACS is preferable to be used in satellite multiple access communication for the same performance of multiple access and better performance of TD and DFS acquisition. Lastly, we conclude the whole letter and there is more significant research in satellite IoT with CSS.

## II. CHANNEL MODEL AND ASYMMETRY CHIRP SIGNAL

### A. Notations

In this letter, we define some notations.  $R_s$  denotes the symbol rate (corresponding symbol period is  $T_s$ , and symbol rate is equal to bit rate in this letter). Transmission bandwidth is  $B$  ( $T = 1/B$ ) and spread factor is  $SF$  ( $SF = 6, 7, 8, \dots, 12$ , in LoRa,  $G = 2^{SF}$ ).  $\mu$  represents the chirp rate,  $\mu_{LCS} = \pm B/T_s$  for LCS,  $\mu_{SA} = \pm 2B/T_s$  for SCS and ACS. The relation between transmission bandwidth and symbol rate is  $BT_s = G$ .  $E_s$  represents the energy of one symbol. The start frequency of CS  $b_k = B_k \cdot B/G$ ,  $B_k \in \{0, 1, 2, 3, \dots, G-1\}$ . We call  $B_k$  as Chirp Number (CN) in this letter.  $B_k^+$  represents the CN of positive chirp rate signal while  $B_k^-$  represents the CN of negative chirp rate signal.  $f_d$  is the value of DFS (Normalized DFS  $F_d = G \cdot f_d/B$ ) and  $\tau$  is the value of TD.

Y. Qian is with Shanghai Institute of Microsystem and Information Technology, Chinese Academy of Sciences, Shanghai 200050, China, and with Shanghai Engineering Center for Microsatellites, Chinese Academy of Sciences, Shanghai 201210, China, and also with University of Chinese Academy of Sciences, Beijing 100049, China. (e-mail: yubiqian@foxmail.com).

L. Ma is with Shanghai SpaceOK Aerospace Technology Co., Ltd., Shanghai 201802, China. (e-mail: e\_wqs@hotmail.com).

X. Liang is with Shanghai Engineering Center for Microsatellites, Chinese Academy of Sciences, Shanghai 201210, China. (e-mail: 18217631362@163.com).

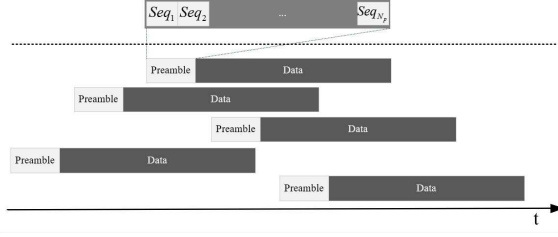


Fig. 1. Structure of Data Frame.

### B. Channel Model

According to Ref. [12], free space path loss (increasing with the increase of carrier frequency) and rain loss are mainly considered in the link budget, and rain loss is severe at above 10 GHz. In addition, the communication between the satellites and terminals needs Line of Sight (LoS) transmission, otherwise it is impossible. In general, the carrier frequency at 1-2GHz is the most suitable for LEO satellite IoT communication in terms of the antenna size, link loss, filter design and so on.

In Fig.1, an example of multi-terminal data packets in time is shown according to PA access protocol. One data packet (LoS transmission) consists of more parts and we only take the sequences (The sequences are composed of  $N_p$  bits of chirp signal) in the preamble and the data part into account [13]. The preamble is used for TD and DFS synchronization while the data part is for transmitting the terminal data. Both of them use the same type of signal for simplifying physical structure. All terminals select the same  $SF$  and random CNs or sequences for data part and the unique CN for preamble part. The received signal is random delay and random frequency offset  $f_d \in \{-B/2, B/2\}$  in Additive White Gaussian Noise (AWGN) channel.

### C. Asymmetry Chirp Signal

In [11], SCS was proposed to decrease the peak value comparing with LCS in terms of TD, but the influence of DFS is ignored because of low data rate and big DFS in satellite communication, which causes big correlation in terms of DFS.

The time-domain SCS ( $B_k^+ = B_k^- = B_k$ ) is expressed as follows,

$$s_k(t) = \sqrt{\frac{E_s}{T_s}} \begin{cases} Se1_k(t), t < T_k^+ \\ (-1)^{B_k^+} Se1_k(t) e^{-j2\pi B t}, t < \frac{T_s}{2} \\ (-1)^{B_k^-} Se2_k(t) e^{j2\pi B t}, t < T_k^- \\ Se2_k(t) e^{j4\pi B t}, t < T_s \end{cases} \quad (1)$$

Where

$$T_k^+ = \frac{(G - B_k^+)T}{2}, T_k^- = \frac{(G + B_k^-)T}{2}$$

$$Se1_k(t) = e^{j2\pi(\frac{B}{T_s}t^2 + b_k^+t)}, Se2_k(t) = e^{j2\pi(-\frac{B}{T_s}t^2 + b_k^-t)}$$

Ambiguity Function (AF) can be expressed as:

$$AF_{k_1, k_2}(\tau, f_d) = \int_{-\infty}^{+\infty} s_{k_1}(t) s_{k_2}^*(t - \tau) e^{-j2\pi f_d t} dt \quad (2)$$

where  $s_i(t)$  is a type of signal for terminal  $i$ . This formula expresses that the correlation of two types of signal in time and frequency domain.

Especially, when  $\tau = 0$ ,  $b_{k_2} > b_{k_1}$ , for SCS,

$$AF_{k_1, k_2}^{SCS}(0, f_d) = \frac{E_s}{T_s} [F(T_{k_2}, 0) + F(\frac{T_s}{2} - T_{k_1}, 0) + F(T_{k_2} - T_{k_1}, B)] \quad (3)$$

where

$$F(\theta, \beta) = 2\theta \frac{\sin[\pi(b_{k_1} - b_{k_2} - f_d - \beta)\theta]}{\pi(b_{k_1} - b_{k_2} - f_d - \beta)\theta}$$

and when  $f_d = b_{k_1} - b_{k_2} - \beta$ ,

$$\max(|F(\theta, f)|) = 2\theta$$

Therefore, when  $f_d^1 = b_{k_1} - b_{k_2}$ ,  $f_d^2 = b_{k_1} - b_{k_2} - B$ , we come to a more general conclusion, not just  $b_{k_2} > b_{k_1}$

$$AF_{k_1, k_2}^{SCS}(0, f_d^1) \approx \frac{G - |B_{k_2} - B_{k_1}|}{G} E_s$$

$$AF_{k_1, k_2}^{SCS}(0, f_d^2) \approx \frac{|B_{k_2} - B_{k_1}|}{G} E_s \quad (4)$$

So, we get the eventual problem:  $\max(|AF_{k_1, k_2}^{SCS}|) \geq 0.5E_s$ , and  $\max(|AF_{k_1, k_2}^{SCS}|) = E_s(G - 1)/G \approx E_s$  when  $|B_{k_2} - B_{k_1}| = 1$  or  $G - 1$ . However, the fundamental factor of big cross-correlation caused by DFS is that  $B_k^+ = B_k^-$ . Hence, according to the traits of SCS, if the hypothesis shown in (5) is true, then the problem can be solved,

$$\begin{cases} T_{k_2}^+ - T_{k_1}^+ \neq T_{k_1}^- - T_{k_2}^- \\ B_{k_2}^+ - B_{k_1}^+ \neq B_{k_2}^- - B_{k_1}^- \end{cases}, B_{k_1}^+ \neq B_{k_2}^+ \quad (5)$$

Based on this hypothesis, several appropriate mapping solutions of  $B_k^-$  and  $B_k^+$  are shown as follows,

$$B_k^- = \begin{cases} (DB_k^+ + 1 - i) \bmod G, D > 0 \\ (DB_k^+ - 2 + i) \bmod G, D < 0 \end{cases} \quad (6)$$

where

$$\frac{Gi}{|D|} \leq B_k^+ < \frac{G(i+1)}{|D|}, i \in \{0, 1, \dots, |D| - 1\}$$

$$|D| = \begin{cases} 2, SF \in \{6, 8, 10, 12\} \\ 3, SF \in \{7, 9, 11\} \end{cases}$$

Eventually, combining (1) and (6), the expression of ACS can be derived.

### III. PERFORMANCE IN RANDOM ACCESS CHANNEL

In this section, we do analysis on the performance of chirp signal in multi-terminal channel. The expression of discrete series is used, and the oversampling period and number of samples in one  $T_s$  are  $T_{sam} = T/M$ ,  $N = M \times G$  respectively. We suppose that TD and DFS have been synchronized perfectly for BER comparison. Combining with binary phase shift keying, we can get,

$$c_k(lT_s^{sf} + nT_{sam}) = a_k(lT_s^{sf} + nT_{sam})s_k(nT_{sam}), \quad (7)$$

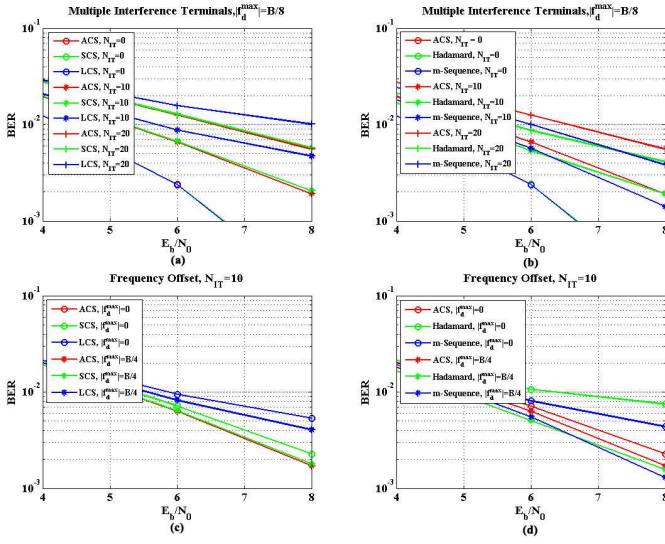


Fig. 2. BER Comparison of ACS, SCS, LCS, Hadamard Matrices and m-Sequences,  $SF = 6$ ,  $M = 2$ .

where  $l \in \{0, 1, 2, \dots, L-1\}$ ,  $n \in \{0, 1, 2, \dots, N-1\}$ ,  $a_k(\cdot)$  and  $c_k(\cdot)$  denote information series  $\{1, -1\}$  with period  $T_s$  and baseband signal with the duration  $LT_s$  for terminal  $k$  respectively. In order to simplify the expression, we get rid of  $T_s, T_{sam}$ . After transmission through the satellite random access channel, we suppose that the received power of all terminals is the same and received baseband signal can expressed as follows according to PA protocol,

$$r(l, n) = \sum_{k=1}^K c_k(l, n - n_k) e^{j2\pi F_d^k n/N} + W(l, n) \quad (8)$$

where  $K$  is the total number of terminals during  $LT_s$ ,  $n_k$  and  $F_d^k$  are normalized TD and DFS respectively,  $n_k \in \{-LN + 1, LN - 1\}$ ,  $r_k(\cdot)$  is received baseband signal and  $W(\cdot)$  is the Gaussian white noise with the variance  $N_0$ . After TD and DFS synchronization ( $n_{k0} = 0$ ), we get,

$$d_{k0}(l) = E_s a_{k0}(l) + \sum_{k \neq k_0} \rho_{k,k_0}(n_k, F_d^k - F_d^{k_0}) + W_{k_0}(l) \quad (9)$$

where

$$W_k(l) = \sum_{n=0}^{N-1} W(l, n) s_k^*(n) e^{j2\pi F_d^k n/N}$$

$$\rho_{k_1, k_2}(n_0, F_d) = \frac{1}{N} \sum_{n=0}^{N-1} (\cdot) e^{j2\pi \frac{F_d n}{N}}$$

$$(\cdot) = a(l, n - n_0) s_{k_2}(n) s_{k_1}^*((n - n_0)_N)$$

In the third equation,  $a(l, n - n_0) = a(l + \lfloor \frac{n - n_0}{N} \rfloor, (n - n_0)_N)$ ,  $\lfloor x \rfloor$  denotes the floor of  $x$  and  $(x)_N$  is the module value of  $N$  divided by  $x$ . Therefore, judge decision is,

$$RE(d_{k_0}(l)) \geq_1^0 0$$

Suppose that real part of  $\rho_{k_1, k_2}$  obeys the normal distribution with zero mean and variance  $N_I$  for random interfered data length, TD and DFS, i.e.  $RE(\rho_{k_1, k_2}) \sim N(0, N_I)$ . So,

Bit Error Rate(BER) function for  $k$  interference terminals can be expressed as,

$$P_e(k) = Q\left(\sqrt{\frac{2E_b}{N_0 + kN_I}}\right) \quad (10)$$

where  $Q(\cdot)$  is Q-function and  $Q(x) = \int_x^{+\infty} \frac{1}{\sqrt{2\pi}} e^{-\frac{t^2}{2}} dt$

From Fig.2, we compare the performance of ACS, SCS, LCS, Hadamard Matrices used in [3] and m-Sequences. When three types of chirp signal are considered in Fig.2(a) and Fig.2(c), the BER performance of ACS is the best under the same situation. For ACS, Hadamard Matrices and m-Sequences in Fig.2(b) and Fig.2(d), the BER performance of ACS is better than that of Hadamard Matrices and m-Sequences when  $|f_d^{max}| = 0$  (DFS is small), but it is worse when  $|f_d^{max}| = B/4$  (DFS is large).

In [14],  $N_I^{DSSS} = 2E_b/3G_s$  for asynchronous direct-sequence spread spectrum multiple access system without DFS ( $G_s$  is spreading gain). Hence, it shows that  $P_e(k)$  is as a function of number of interference terminals  $k$ , spreading gain  $G_s$ , and the energy per bit to noise power spectral density ratio  $E_b/N_0$ . For different kinds of Chirp signal with the existence of DFS, we can use approximate estimation methods to obtain their BER functions through modifying the coefficient of  $N_I$ .

#### IV. ACQUISITION PERFORMANCE OF TIME DELAY AND DOPPLER FREQUENCY SHIFT

##### A. Traits of Three Types of Chirp Signal and DSSS Signal

According to (2), we give the traits of LCS, SCS, ACS and DSSS signal at the peak value,

- When  $s_k(t)$  is DSSS signal, its maximum AF at  $\tau = 0$  is,

$$|AF_k^{DSSS}(0, f_d)| = E_s \left| \frac{\sin(\pi f_d T_s)}{\pi f_d T_s} \right| \quad (11)$$

The first zero is at  $f_d = \pm \frac{1}{T_s} = \pm \frac{B}{G}$ , which means that its AF is smaller when absolute DFS is more than  $\frac{B}{G}$ .

- When  $s_k(t)$  is LCS, then we can get its maximum AF at  $\tau^* = f_d/\mu_{LCS}$ ,

$$|AF_k^{LCS}(\tau^*, f_d)| = E_s \begin{cases} 1 - |\frac{2f_d}{B}|, B_k \neq 0 \\ 1 - |\frac{f_d}{B}|, B_k = 0 \end{cases} \quad (12)$$

- When  $s_k(t)$  is SCS or ACS, then we can get their maximal AF at  $\tau^* = f_d/\mu_{SA}$  and  $-f_d/\mu_{SA}$ ,

$$|AF_k^{SA}(\tau^*, f_d)| \approx \frac{E_s}{2} \begin{cases} 1 - |\frac{2f_d}{B}|, B_k \neq 0 \\ 1 - |\frac{f_d}{B}|, B_k = 0 \end{cases} \quad (13)$$

- When  $s_{k_1}(t)$  is SCS or ACS and  $s_{k_2}(t)$  is DSSS signal, then for arbitrary  $\tau$  and  $f_d$ , we find

$$|AF_{k_1, k_2}^{SA, DSSS}(\tau, f_d)| \approx 0 \quad (14)$$

In LEO satellite IoT, symbol rate ( $1/T_s$ ) is several hundred bits per second and maximum DFS is much bigger than the symbol rate. Through comparing with (11), (12) and (13), the anti-frequency-offset capacity of LCS is the best and that of DSSS signal is the worst. In other words, chirp signal can find the peak value through changing TD and the peak value is bigger as  $B$  is bigger, like Extended Matched Filter Method [9]

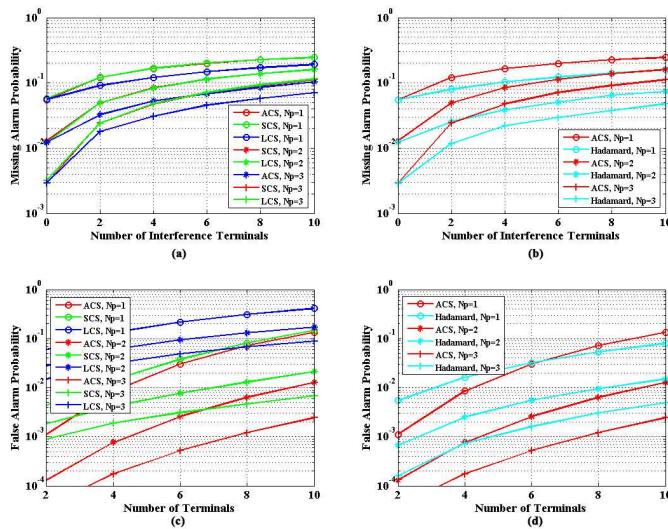


Fig. 3. MAP and FAP of ACS, SCS, LCS and Hadamard Matrices,  $SF = 6$ ,  $M = 2$ ,  $E_b/N_0 = 15dB$ ,  $\lambda_{th} = 0.8$ ,  $D = -2$ ,  $f_d^{max} = -B/8$ .

and Fast Acquisition Approach [10]. But for DSSS signal, it is difficult to do with this way. Hence, Chirp signal is easier to be captured with the existence of TD and large DFS, which is the key factor that CSS is a method of low-power-consumption modulation. According to (14), the correlation between SCS (ACS) and DSSS signal is very small, which means that CSS has better anti-interference capacity.

### B. Acquisition Performance of SCS, ACS and LCS

In Section II, the received signal that can be demodulated is based on perfect TD and DFS synchronization. The simplest method to capture TD and DFS is to find the peak value (more than given threshold  $\lambda_{th}E_s$ ) through searching frequency offset or using fast Fourier transform [15] in each sampling point.

According to Fig.1, when detecting the sequences for TD and DFS acquisition, it will be interfered from the data part of other terminals. Hence, there are two kinds of alarm probability at a certain time point in AWGN channel,

- **Missing Alarm Probability (MAP):** Detected decision for the sequences isn't a preamble while the sequence is actually a preamble.
- **False Alarm Probability (FAP):** Detected decision for the sequences is a preamble while the sequence is actually the data part.

We give the acquisition simulations with Monte Carlo method shown in Fig.3. For MAP, the performance of LCS and Hadamard Matrices are better than that of SCS and ACS. For FAP, the performance of ACS is the best comparing with the others. On the whole, the acquisition performance of ACS is better than that of SCS and LCS. Besides, MAP and FAP of them are as smaller as  $N_p$  increasing.

## V. CONCLUSION

This letter is on the research of performance of SCS, ACS and LCS in LEO satellite communication system for IoT. ACS

has great auto-correlation and better cross-correlation in time and frequency domain, so ACS is the best chirp signal to be used in LEO satellite IoT in terms of BER and acquisition performance. In addition, we don't do deep research on the acquisition and we will focus on the acquisition method of ACS in further research.

## REFERENCES

- [1] P. K. Chowdhury, M. Atiquzzaman, and W. Ivancic, Handover schemes in satellite networks: State-of-the-art and future research directions, IEEE Commun. Surveys Tuts., vol. 8, no. 4, pp. 2C14, 4th Quart., 2006. <http://www.etsi.org>.
- [2] Del Rio Herrero, O. De Gaudenzi, R. High Efficiency Satellite Multiple Access Scheme for Machine-to-Machine Communications. IEEE TRANSACTIONS ON AEROSPACE AND ELECTRONIC SYSTEMS, VOL. 48, NO. 4, PP. 2961 - 2989, OCTOBER 2012.
- [3] ETSI, Satellite Earth Stations and Systems (SES); Air Interface for S-band Mobile Interactive Multimedia (S-MIM); Part 4: Physical Layer Specification, Return Link Synchronous Access. Available:
- [4] Lorenzo Vangelista. Frequency Shift Chirp Modulation: The LoRa Modulation. IEEE SIGNAL PROCESSING LETTERS, VOL. 24, NO. 12, PP. 1818-1821, December 2017.
- [5] LoRaWan, <https://lora-alliance.org/sites/default/files/2018-04/lorawantm-specification-v1.1.pdf>, 2018, accessed:2018-10.
- [6] Daegun Oh, Myungkyun Kwak, and Jong-Wha Chong. A Subspace-Based Two-Way Ranging System Using a Chirp Spread Spectrum Modem, Robust to Frequency Offset. IEEE TRANSACTIONS ON WIRELESS COMMUNICATIONS, VOL. 11, NO. 4, APRIL 2012.
- [7] Teng Wang ; Hao Huan ; Chuying Feng ; Ran Tao. Chirp Noise Waveform Aided Fast Acquisition Approach for Large Doppler Shifted TT&C System. 2015 IEEE Global Communications Conference (GLOBECOM), PP. 1- 6.
- [8] H. Wang and A. O. Fapojuwo. A survey of enabling technologies of low power and long range machine-to-machine communications. IEEE Commun. Surv. VOL. 19, NO. 4, PP.2621 - 2639, FOURTH QUARTER 2017.
- [9] Ravi Kadlimatti, Adly T. Fam. Doppler Detection for Linear FM Waveform Using Extended Matched Filter. 2016 IEEE Radar Conference, PP. 1-5.
- [10] Teng Wang ; Hao Huan ; Chuying Feng ; Ran Tao. Chirp Noise Waveform Aided Fast Acquisition Approach for Large Doppler Shifted TT&C System. 2015 IEEE Global Communications Conference (GLOBECOM), PP. 1- 6.
- [11] Yubi Qian; Lu Ma; Xuwen Liang. Symmetry Chirp Spread Spectrum Modulation used in LEO Satellite Internet of Things. IEEE COMMUNICATIONS LETTERS, VOL. 22, NO. 11, PP.2230-2233, NOVEMBER 2018.
- [12] Kundu A K, Khan M T H, Sharmin W, et al. Designing a mobile satellite communication antenna and link budget optimization[C]. International Conference on Electrical Information & Communication Technology. IEEE, 2014.
- [13] Li Zhen, Hao Qin, Bin Song, Rui Ding, Xiaojiang Du, Mohsen Guizani. Random Access Preamble Design and Detection for Mobile Satellite Communication Systems. IEEE Journal on Selected Areas in Communications, IEEE JOURNAL ON SELECTED AREAS IN COMMUNICATIONS, VOL. 36, NO. 2, PP. 280-291, FEBRUARY 2018.
- [14] T. Yamazato, T. Sato, K. Okada, M. Katayama, A. Ogawa. Throughput and delay analysis of DS/SSMA unslotted ALOHA by non-perfect capture. Proceedings of ICUPC '95 - 4th IEEE International Conference on Universal Personal Communications, August 2002.
- [15] Ping Huang, Bing-Fa Zu. Performance Analysis of PN Code Acquisition Using Fast Fourier Transform. 2009 5th International Conference on Wireless Communications, Networking and Mobile Computing, October, 2009.